Improving the Prediction of the Summer Asian–Pacific Oscillation Using the Interannual Increment Approach

YANYAN HUANG

Nansen-Zhu International Research Centre, Institute of Atmospheric Physics, Chinese Academy of Sciences, University of the Chinese Academy of Sciences, and Climate Change Research Center, Chinese Academy of Sciences, Beijing, China

HUIJUN WANG

Nansen-Zhu International Research Centre, Institute of Atmospheric Physics, and Climate Change Research Center, Chinese Academy of Sciences, Beijing, China

KE FAN

Nansen-Zhu International Research Centre, Institute of Atmospheric Physics, Chinese Academy of Sciences, Beijing, and Collaborative Innovation Center on Forecast and Evaluation of Meteorological Disasters, Nanjing University of Information Science and Technology, Nanjing, China

(Manuscript received 18 March 2014, in final form 18 June 2014)

ABSTRACT

The summer Asian–Pacific oscillation (APO) is a dominant teleconnection pattern over the extratropical Northern Hemisphere that links the large-scale atmospheric circulation anomalies over the Asian–North Pacific Ocean sector. In this study, the direct Development of a European Multimodel Ensemble System for Seasonal-to-Interannual Prediction (DEMETER) model outputs from 1960 to 2001, which are limited in predicting the interannual variability of the summer Asian upper-tropospheric temperature and the decadal variations, are applied using the interannual increment approach to improve the predictions of the summer APO. By treating the year-to-year increment as the predictand, the interannual increment scheme is shown to significantly improve the predictive ability for the interannual variability of the summer Asian upper-tropospheric temperature and the decadal variations. The improvements for the interannual and interdecadal summer APO variability predictions in the interannual increment scheme relative to the original scheme are clear and significant. Compared with the DEMETER direct outputs, the statistical model with two predictors of APO and sea surface temperature anomaly over the Atlantic shows a significantly improved ability to predict the interannual variability of the summer rainfall over the middle and lower reaches of the Yangtze River valley (SRYR). This study therefore describes a more efficient approach for predicting the APO and the SRYR.

1. Introduction

Current climate models employed to predict the Asian summer monsoon still perform at a low level, especially for the monsoon rainfall. Their limited skill has been attributed to the unstable relationship with El Niño–Southern Oscillation (ENSO) (Wang 2002; Feng et al. 2011; X. Wang et al. 2012), model systematic bias (Ma et al. 2012), and the poor performance of the decadal change–related circulation (Fan et al. 2012).

Recently, Zhao et al. (2007) reported that the summer upper-tropospheric temperature over Asia is teleconnected with temperature over the North Pacific, an effect known as the Asian–Pacific oscillation (APO). A positive (negative) APO phase corresponds to a higher (lower) tropospheric temperature over Asia and a lower (higher) tropospheric temperature over the North Pacific and indicates a strengthened (weakened) thermal contrast between Asia and the North Pacific (Zhao et al. 2012). It has been demonstrated that the interannual variability of

Corresponding author address: Yanyan Huang, Institute of Atmospheric Physics, Chinese Academy of Sciences, Nansen-Zhu International Research Centre, 40 Huayanli, Chaoyang District, Beijing 100029, China.
E-mail: hyy@mail.iap.ac.cn

DOI: 10.1175/JCLI-D-14-00209.1

the summer APO is closely associated with Asian summer climate anomalies such as the South Asian high, the western Pacific subtropical high, the tropical easterly jet, and the Asian summer monsoon and rainfall (Zhao et al. 2007; Zhou and Zhao 2010; Zhao et al. 2012). Based on the close relationship between the APO and the Asian summer monsoon, Huang et al. (2013) investigated the predictability of the APO interannual variability to gain new insights into Asian summer monsoon prediction. They used three coupled ocean–atmosphere models from the Development of a European Multimodel Ensemble System for Seasonal-to-Interannual Prediction (DEMETER) project (Palmer et al. 2004). Their results showed that the DEMETER general circulation models (GCMs) could reasonably predict the APO interannual variability. However, the GCMs had higher skill for the North Pacific than for the Asian upper-tropospheric temperature and failed to predict the decadal variations.

Compared to the conventional prediction approach, which focuses on predicting the anomalies of a variable relative to climatology, a new interannual increment approach that treats the year-to-year increment of a variable (i.e., the difference in the variable between the current year and the previous year, called DY) as the predictand was recently applied in the short-term climate prediction researches (H. Wang et al. 2012). This interannual increment approach produced the final predicted variable by adding the predicted DY of the variable to the observed value from the previous year. The rationality of this approach is based on the tropospheric biennial oscillation (TBO) feature of climate variables, such as the Asian monsoon, the rainfall and temperature over eastern China, and other climatic factors. Considering the contribution of the TBO to a climate variable, if f_i represents the anomaly of a variable in the current year, and likewise f_{i-1} the previous year, then $f_i = C + P_i$ and $f_{i-1} = -C + P_{i-1}$, where P_i and P_{i-1} represent a disturbance in C, and $f_i \approx C$ and $\mathrm{DY} = f_i - f_{i-1} \approx 2C$, suggesting that the amplitude of a variable in the form of the year-to-year increment is twice the value of the anomaly. Thus, treating the interannual increment of a variable as the predictand can amplify the prediction signals (Wang et al. 2010). On the other hand, because the previous year's observed value of the variable should be inherently realistic, and contains the interdecadal variations of the variable, the interannual increment approach is advantageous in capturing the interdecadal variability of the variable (Fan et al. 2012). It has been demonstrated that the interannual increment approach can significantly improve the prediction of summer rainfall in eastern China (Fan et al. 2008), temperature in northeastern China (Fan 2009), activity of western North Pacific typhoons (Fan and Wang 2009), Atlantic hurricanes (Fan 2010), and the East Asian summer monsoon (Fan et al. 2012).

Considering the limited skill of the DEMETER GCMs in predicting the Asian upper-tropospheric temperature and the decadal variations, there is substantial room for enhancing the APO prediction. In this study, we apply the interannual increment approach to the DEMETER hindcasts to improve the predictions for the Asian upper-tropospheric temperature and to further try to improve the APO prediction. Moreover, based upon the close relationship between the APO and the East Asian monsoon rainfall, improving the prediction of summer rainfall over the middle and lower reaches of the Yangtze River valley (SRYR) is also considered using the improved APO hindcasts.

The remainder of the paper is organized as follows. The data and analysis methods applied are introduced in section 2. Section 3 describes the predictive skills of DEMETER GCMs with regard to summer APO variations. In section 4, we apply the interannual increment approach to the DEMETER hindcasts to improve the APO prediction. Further improvements to the performance of the DEMETER GCMs in predicting the SRYR is described in section 5. Finally, a summary and possible reasons for the improved ability of the interannual increment approach are given in section 6.

2. Data and method

Following Huang et al. (2013), three coupled ocean–atmosphere DEMETER GCMs with hindcast data for the period 1959–2001, initiated on 1 May, are analyzed in this study. The coupled ocean–atmosphere models are those developed by the European Centre for Medium-Range Weather Forecasts (ECMWF), the Centre National de Recherches Météorologiques (CNRM), France, and the Met Office (UKMO), United Kingdom (Palmer et al. 2004). The multimodel ensemble (MME) is calculated as the simple average of the ECMWF, CNRM, and UKMO hindcasts. In addition, the monthly 40-yr ECMWF Re-Analysis (ERA-40) data (Uppala et al. 2005) are used as a verification dataset. The observed precipitation data are derived from the CN05.1 dataset, based upon over 2400 station observations in China (Wu and Gao 2013). We focus our analysis solely on the summer months of June–August (JJA).

The model's predictive skill is tested using the time correlation coefficient (CC) between the observation and the model prediction, as well as the root-mean-square error (RMSE). Additionally, a multivariate regression method is used to build a statistical model to predict SRYR. The predictive capability of the statistical model is assessed using one-year-out cross-validation

(Michaelsen 1987). The cross-validation method excludes one year of data during the period 1961–2001 when constructing the statistical model, and subsequently uses the model to predict the year of the excluded data. The statistical significance is assessed using a Student's t test.

3. The predictive skill of DEMETER models

Following Zhao et al. (2007), the eddy air temperature T' is used to calculate the APO index, in which $T' = T - \overline{T}$, where T is the total air temperature and $\overline{T}$ is the zonal mean (symmetric) temperature. In particular, we define the Asian tropospheric temperature index (AI) and the North Pacific tropospheric temperature index (PI) as the regionally averaged upper-tropospheric (500–200 hPa) T' over 15°–50°N, 60°–120°E and 15°–50°N, 180°–120°W, respectively. The APO index is defined as the arithmetic difference between the AI and PI.

Figure 1 displays the summer AI and the DY of AI from 1960 to 2001 for ERA-40 and the GCMs. The CCs between the predicted and observed AI are 0.23, 0.06, and 0.27 for the CNRM and UKMO models and the multimodel ensemble (MME), respectively (Table 1). None of the CCs is statistically significant, indicating the low ability of the DEMETER GCMs to predict the AI. Meanwhile, the ECMWF model, which has a CC of 0.31, significant at the 95% confidence level, displays skill in predicting the AI. In addition, all the DEMETER GCMs and the MME are unable to capture the observed decreasing trend of the AI, an effect that may contribute to the weakening of the East Asian summer monsoon (Wang 2001) (Fig. 1a). The CCs for the DY of AI are 0.41 (significant at the 99% confidence level), 0.29 (significant at the 94% confidence level), 0.41 (significant at the 99% confidence level), and 0.49 (significant at the 99.9% confidence level) for the CNRM, UKMO, and ECMWF models and for the MME, respectively (Table 1), which are apparently higher than the CCs for the original AI form, indicating that the DEMETER GCMs have better skill in predicting the DY of AI than for the original form (Fig. 1b).

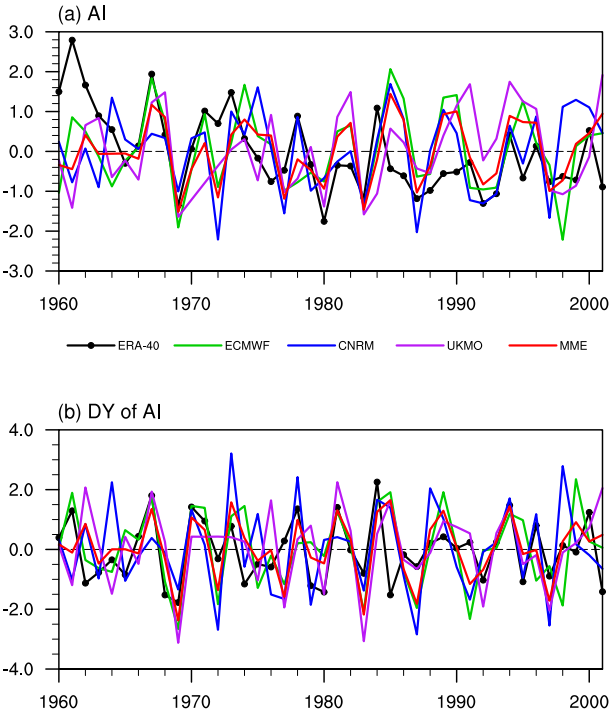

FIG. 1. The normalized (a) JJA AI and (b) DY of AI for the years 1960–2001 for ERA-40 (black line with dots), the ECMWF model (green line), the CNRM model (blue line), the UKMO model (purple line), and the MME (red line).

The CCs for the PI (DY of PI) in the UKMO model and the MME are 0.60 (0.72) and 0.63 (0.67), all significant at the 99.9% confidence level. These results show that the models have a greater ability to predict PI in the form of DY than in the original PI form. Meanwhile, the CNRM and ECMWF models display good comparable skill in both PI and DY of PI predictions. (Table 1; figure not shown). Additionally, the DEMETER GCMs perform very poorly in predicting the increasing decadal trend of PI in ERA-40 (not shown).

The predicted and observed APO and DY of APO for 1960–2001 are shown in Fig. 2. The CCs for the APO (DY of APO) are 0.43 (0.51), 0.46 (0.66), 0.49 (0.51), and 0.52 (0.64) for CNRM, UKMO, ECMWF, and MME, respectively (Table 1). With the better performance for

TABLE 1. The CCs between the observed and direct predicted AI, PI, and APO (and the corresponding DY form in parentheses) in the DEMETER GCMs during 1960–2001 along with the RMSE. Boldface numbers are significant at the 95% confidence level.

	Correlation coefficient of			Root-mean-square error of		
	AI	PI	APO	AI	PI	APO
CNRM	0.23 (**0.41**)	**0.56** (**0.51**)	**0.43** (**0.51**)	1.23	0.94	1.06
UKMO	0.06 (0.29)	**0.60** (**0.72**)	**0.45** (**0.66**)	1.36	0.90	1.05
ECMWF	**0.31** (**0.41**)	**0.55** (**0.50**)	**0.49** (**0.51**)	1.16	0.95	1.01
MME	0.27 (**0. 49**)	**0.63** (**0.67**)	**0.52** (**0.64**)	1.20	0.86	0.97

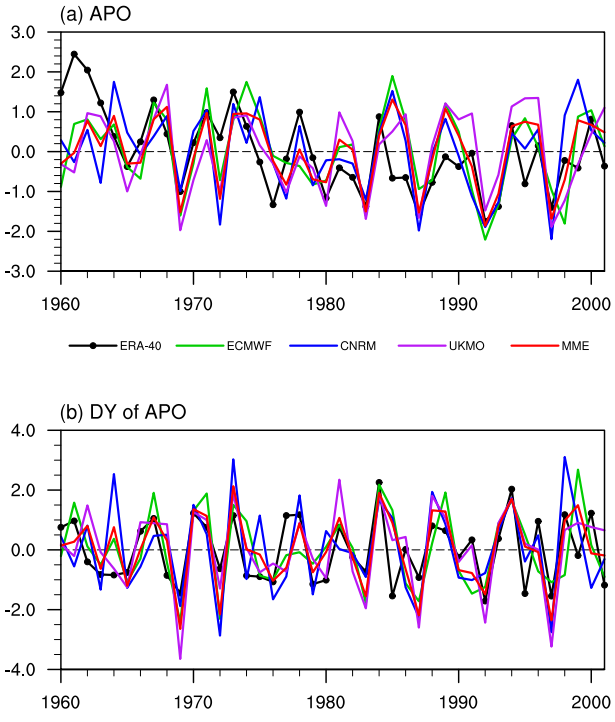

FIG. 2. As for Fig. 1, but for the APO index.

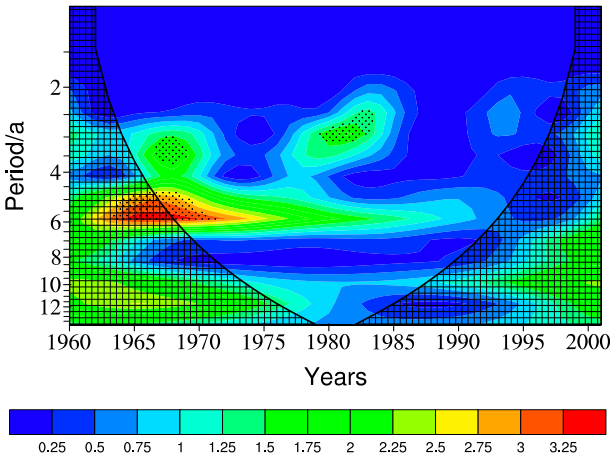

FIG. 3. Wavelet analysis of the JJA AI for the period 1960–2001. The dotted regions indicate significant variability at the 95% significance level estimated by a red noise process, and the parabola indicates the "cone of influence."

the DY of AI and DY of PI, especially for the former, the DEMETER GCMs show higher skill for the DY of APO form than for the original APO form, implying that the interannual increment approach is feasible for further improving the APO prediction. However, the DEMETER GCMs also fail to predict the observed weakening trend of the APO (Fig. 2a).

4. The interannual increment prediction approach for the AI, PI, and APO

Besides of the higher skill of the DEMETER GCMs to predict in the DY form than in the original form, especially for the AI, wavelet analysis shows that the TBO is a significant feature of the AI during 1960–2001 (Fig. 3) as well as the PI (not shown), and consequently the interannual increment approach is applied to the AI and PI in this section. The predicted APO index is obtained from the arithmetic difference between the predicted AI and PI. Particularly, the predicted AI is obtained by adding the DY of AI derived from the model's current year output to the observed AI value in the previous year; that is, $\hat{y}_i = x_i + y_{i-1}$, where $\hat{y}_i$ is the predicted AI for each model, x_i is the DY of AI derived from the direct output of each model, and y_{i-1} is the observed AI from the previous year. The predicted PI is calculated in the same way.

The predicted AIs obtained from the interannual increment approach are shown in Fig. 4a. The CCs for the interannual increment scheme (hereafter CCs-DY) of the AI are 0.51, 0.53, 0.58, and 0.63, all significant at the 99.9% confidence level for the CNRM, UKMO, and ECMWF models and for the MME, respectively. These values are substantially higher than the CCs for the old scheme (0.23, 0.06, 0.31, and 0.27, respectively) (Table 2). The percentage improvement in the RMSEs for the interannual increment scheme are 21%, 29%, 22%, and 30% for the CNRM, UKMO, and ECMWF models and for the MME, respectively (Table 2). This indicates that the AI can able to be better predicted when the interannual increment scheme is applied to the DEMETER GCM

TABLE 2. The CCs between observed and predicted AI, PI, and APO through the interannual increment approach in DEMETER GCMs during 1960–2001 along with the RMSE for the interannual increment approach (improvement in RMSE in parentheses). Boldface numbers are significant at the 95% confidence level.

	Correlation coefficient of			Root-mean-square error of		
	AI	PI	APO	AI	PI	APO
CNRM	**0.51**	**0.53**	**0.57**	0.97 (21%)	0.97 (−3%)	0.92 (13%)
UKMO	**0.53**	**0.75**	**0.72**	0.96 (29%)	0.70 (22%)	0.75 (29%)
ECMWF	**0.58**	**0.59**	**0.63**	0.90 (22%)	0.90 (6%)	0.85 (15%)
MME	**0.63**	**0.71**	**0.72**	0.85 (30%)	0.76 (11%)	0.75 (23%)

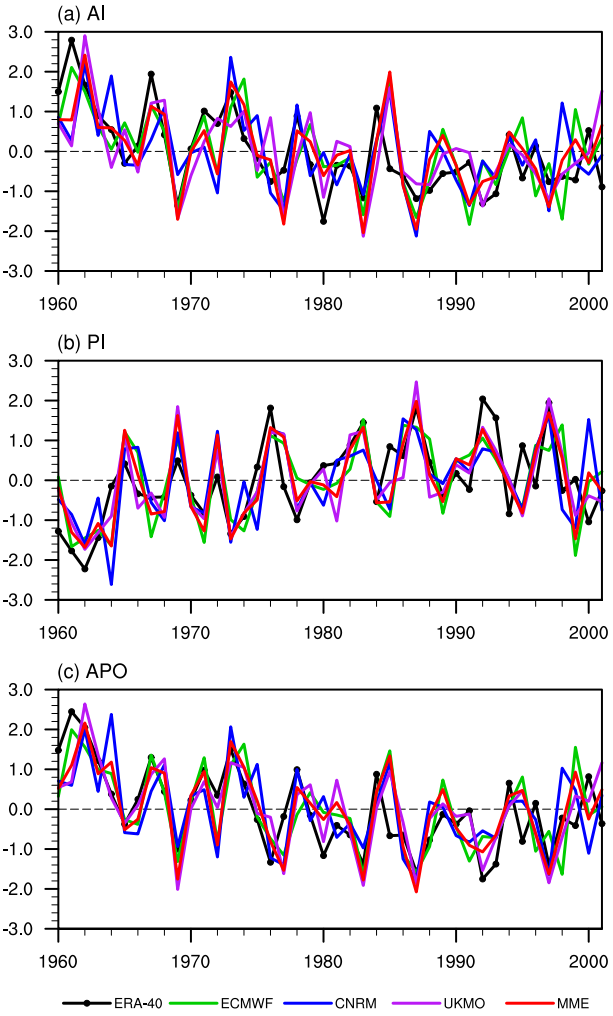

FIG. 4. The predicted (a) AI, (b) PI, and (c) APO using the interannual increment approach for ERA-40 (black line with dots), the ECMWF model (green line), the CNRM model (blue line), the UKMO model (purple line), and the MME (red line).

hindcasts. In addition, all of the DEMETER GCMs successfully predict the decreasing decadal trend of the AI with a positive phase before 1975 and a negative phase afterward.

Figure 4b shows the interannual increment scheme predicted PI during 1960–2001. The CCs-DY (CCs) of the PI are 0.75 (0.60), 0.59 (0.55), and 0.71 (0.63) for the UKMO and ECMWF models and the MME, respectively. The percentage improvement in the RMSE of the PI for the UKMO and ECMWF models and the MME for the interannual increment scheme are 22%, 6%, and 11% (Table 2), respectively. These results again illustrate the ability of the interannual increment approach to improve PI prediction in comparison with the old scheme. However, the improvement for the interannual increment approach in PI prediction is not significant for the CNRM model results, which has a slightly lower CC-DY of 0.53 (0.56 for the old scheme) and a slightly larger RMSE of 0.97 (0.94 for the old scheme). Furthermore, all the DEMETER GCMs successfully capture the observed increasing decadal trend in the PI after applying the interannual increment approach.

Figure 4c illustrates the predicted APOs for the GCMs obtained from the arithmetic difference between the predicted AI and PI through the interannual increment approach. In comparison with the CCs for the old scheme, which have CCs of 0.43, 0.45, 0.49, and 0.52 for the CNRM, UKMO, and ECMWF models and for the MME, the CCs-DY of the APO are 0.57, 0.72, 0.63, and 0.72, respectively. The RMSEs for the interannual increment scheme of the APO are reduced by 13%, 29%, 15%, and 23% for the CNRM, UKMO, and ECMWF models and for the MME (Table 2), respectively. The improved ability of the interannual increment approach is significant in the APO results. Furthermore, as shown in Fig. 4c, all the GCMs perform well in predicting the observed weakening decadal trend of the APO in the interannual increment scheme.

5. Improving the prediction of summer rainfall over the SRYR

A larger variability with the occurrence of extreme floods and droughts is a characteristic feature of the SRYR (e.g., Zhao 1999; Zhu et al. 2011; Li et al. 2012). Predicting SRYR is therefore tied up with socioeconomic development in China. However, the current predictive skill of many models is still limited in this region (Sun and Chen 2012; Chen at al. 2012). Based upon the close relationship between the APO and the SRYR (cf. Zhao et al. 2007, their Fig. 12a), the improved APO predictions discussed in section 4 are applied to improve the prediction of the SRYR.

Figure 5a displays the SRYR during 1961–2001 for the observations and the GCM results, in which the SRYR is defined as the summer rainfall averaged over 27.5°–32.5°N, 110°–122.5°E. The CCs between the observed and predicted SRYR have values of 0.21, −0.03, 0.23, and 0.14 for the CNRM, UKMO, and ECMWF models and the MME (Table 3), respectively, that are not statistically significant, indicating the poor skill of the DEMETER GCMs in predicting the SRYR.

To improve prediction of SRYR, we build a statistical model to predict the SRYR with two predictors based on multivariate regression:

$$\mathrm{SRYR} = a\mathrm{APO} + b\mathrm{SSTA}_{\mathrm{Atlantic}}. \quad (1)$$

Here APO denotes the improved APO index obtained by the interannual increment approach in DEMETER

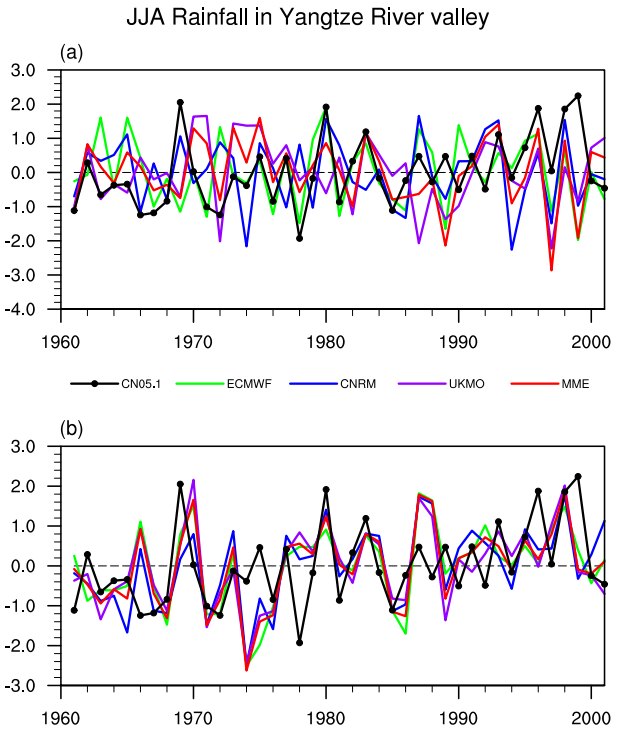

FIG. 5. (a) The normalized JJA rainfall over the SRYR (27.5°–32.5°N, 110°–122.5°E) during 1961–2001 for the CN05.1 dataset (black line with dots), the ECMWF model (green line), the CNRM model (blue line), the UKMO model (purple line), and the MME (red line). (b) As in (a), but for the predicted SRYR using the statistical model in the cross-validation.

GCM, $SSTA_{Atlantic}$ is the model-predicted summer mean sea surface temperature anomaly (SSTA) averaged over the Atlantic region (0°–20°N, 50°–20°W). The coefficients a and b are regression coefficients obtained from the multivariate regression analysis using the observed data. These predictors are chosen since they have significant CCs with the SRYR (−0.40 for APO and 0.52 for $SSTA_{Atlantic}$) and they are well predicted by DEMETER GCMs (Tables 2 and 3). Physically, in addition to the APO, the SSTA over the Atlantic can greatly influence the East Asian summer climate through exciting anomalous wavelike patterns (Gu et al. 2009; Sun et al. 2009; Bothe et al. 2011; Gao et al. 2013) and impacting the ENSO–monsoon relationship (Rong et al. 2010).

The predictive ability of this statistical model is tested using the cross-validation method with a 1-year-out approach. Figure 5b shows the SRYR predicted by the statistical model in the cross-validation procedure. The CCs of SRYR for the observations and in the cross-validations reach 0.42 (significant at the 99% confidence level), 0.33 (significant at the 95% confidence level), 0.34 (significant at the 95% confidence level), and 0.38 (significant at the 95% confidence level) for the CNRM, UKMO, and ECMWF models and the MME (Table 4), respectively. Meanwhile, compared with the original scheme, the RMSEs for the SRYR in the cross-validation are reduced by 14%, 20%, 9%, and 15% for the CNRM, UKMO, and ECMWF models and the MME (Table 4), respectively. The skills of the DEMETER GCMs in predicting the interannual variability of the SRYR are improved significantly by using the statistical model.

TABLE 3. The CCs between the observed and predicted $SSTA_{Atlantic}$ in DEMETER GCMs during 1961–2001. All numbers are significant at the 95% confidence level.

CNRM	UKMO	ECMWF	MME
0.80	0.68	0.79	0.79

6. Conclusions and discussion

The Asian–Pacific oscillation is a large-scale teleconnection over the Asian–North Pacific sector and is closely associated with the atmospheric circulation anomalies over the Northern Hemisphere and with sea surface temperature (Zhao et al. 2010; Zhou et al. 2010) and the tropical typhoon frequency in the western North Pacific (Zhou at al. 2008). In this study, we assess the predictive ability of the APO during 1960–2001 in three DEMETER GCMs (CNRM, UKMO, and ECMWF) and apply the interannual increment approach to the model hindcasts to improve the APO prediction. We then further improve the predictions of the DEMETER GCMs for the summer rainfall over the middle and lower valley of the Yangtze River (SRYR).

Although the DEMETER GCMs have the ability to predict the interannual variability of the APO and the North Pacific upper-tropospheric temperature (PI), the CNRM and UKMO models and the MME, which have insignificant correlation coefficients (CCs) and large root-mean-square errors (RMSEs), display no skill in predicting the interannual variability of the Asian upper-tropospheric temperature (AI). Meanwhile, the DEMETER GCMs fail to predict the observed

TABLE 4. The CCs between the observed and predicted SRYR by the statistical model in the cross-validation (in DEMETER direct outputs) during 1961–2001 along with the RMSE (improvement of RMSE in parentheses). Boldface numbers are significant at the 95% confidence level.

	CC	RMSE
CNRM	**0.42** (0.21)	1.07 (14%)
UKMO	**0.35** (−0.03)	1.12 (20%)
ECMWF	**0.34** (0.23)	1.14 (9%)
MME	**0.38** (0.14)	1.10 (15%)

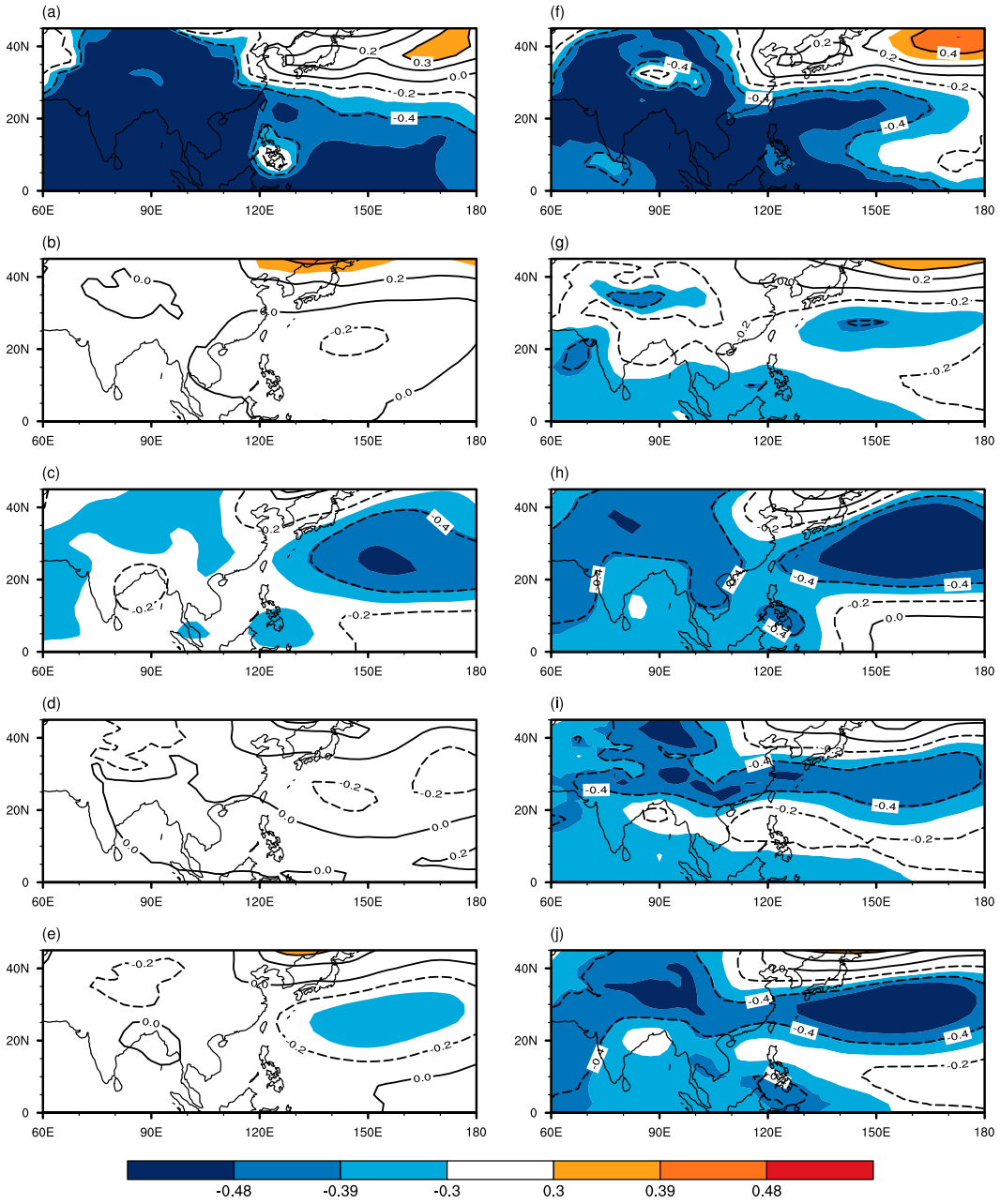

FIG. 6. The CCs between the observed AI and H850 during 1960–2001 for (a) ERA-40, (b) the ECMWF model, (c) the CNRM model, (d) the UKMO model, and (e) the MME. (f)–(j) As in (a)–(e), but for the CC between the observed DY of AI and the DY of H850. Dark, medium, and light blue and red–orange shading in (a) and (b) indicate significance at the 99.9%, 99% and 95% confidence levels, respectively, using a Student's *t* test.

decreasing, increasing, and weakening trends for the AI, PI, and APO, respectively. However, the DEMETER GCMs show good skill for the DY of AI, and better performance is also observed for the DY of PI in the UKMO model and in the MME. Therefore, we apply the interannual increment approach to the AI and PI to improve the skill in predicting the AI and PI. The predicted APO index is obtained from the arithmetic difference between the predicted AI and PI. The improvements for the AI and PI predictions in the interannual increment approach relative to the original approach are significant. In particular, the CCs of the AI increase significantly, and the RMSEs are reduced. The CCs for the PI also increase, and reductions in RMSEs are also seen. Accordingly, the CCs of APO increase with significant reductions in RMSE (Table 2).

Furthermore, when the interannual increment approach is applied to the model hindcasts, the DEMETER GCMs successfully capture the decadal decreasing, increasing, and weakening trends of the AI, PI, and APO, respectively, indicating the improved ability of the interannual increment approach for the APO prediction.

The statistical model with two predictors of APO and sea surface temperature over the Atlantic shows a significantly improved ability in predicting the interannual variability of the SRYR during the 1961–2001 period. The CCs between the observed and predicted SRYR increase and reductions in the RMSE are seen for all models (Table 4).

There may be two reasons for the better performance of the DEMETER GCMs in predicting in the DY form than the original form. First, the larger variance of the DY of the variable compared with the variance of the original variable may lead to better predictions (Sun and Wang 2013). The variances of AI (DY of AI) are 1.02 (2.21), 1.02 (1.67), 1.0 (1.68), and 1.01 (1.83) for the CNRM, UKMO, and ECMWF models and for the MME, respectively. The variances of PI (DY of PI) are 1.02 (2.02), 1.02 (2.11), 1.02 (1.55), and 1.02 (1.86) for the CNRM, UKMO, and ECMWF models and for the MME, respectively. Second, it may be attributed to the better performance of the DEMETER GCMs in predicting the DY of the circulation anomalies associated with the DY of AI because of the amplified prediction signals in the DY form. Figure 6a shows that the observed AI is significantly and negatively correlated with the geopotential height at 850 hPa (H850) from low-latitude Eurasia to the western Pacific, indicating a stronger Asian low and weakened western Pacific subtropical high when the AI is above normal. However, the ECMWF and UKMO models and the MME fail to capture the H850 circulation anomalies associated with the observed AI (Figs. 6b–e). Although the CNRM model reproduces the negative correlation over the western Pacific, the correlation coefficient over low-latitude Eurasia is underestimated by the CNRM model. Meanwhile, the DEMTER GCMs show good ability to predict the linkage between the DY of AI and the DY of H850. In particular, each model successfully reproduces a strong Asian low and a weakened western Pacific subtropical high over the study region associated with an observed positive AI phase (Figs. 6g–j). Similar features are also observed in the correlation map between the observed AI and the 500-hPa geopotential height (not shown). Moreover, better performance for the DY of the circulation anomalies associated with the DY of PI and APO in DEMETER GCMs is also observed (not shown).

Acknowledgments. This research was supported by the National Natural Science Foundation of China (Grants 41130103 and 41210007).

REFERENCES

Bothe, O., K. Fraedrich, and X. Zhu, 2011: Large-scale circulations and Tibetan Plateau summer drought and wetness in the high-resolution climate model. *Int. J. Climatol.,* **31,** 832–846, doi:10.1002/joc.2124.

Chen, H., J. Sun, and H. Wang, 2012: A statistical downscaling model for forecasting summer rainfall in China from DEMETER hindcast datasets. *Wea. Forecasting,* **27,** 608–628, doi:10.1175/WAF-D-11-00079.1.

Fan, K., 2009: Predicting winter surface air temperature in northeast China. *Atmos. Oceanic Sci. Lett.,* **2,** 14–17.

——, 2010: A prediction model for Atlantic named storm frequency using a year-by-year increment approach. *Wea. Forecasting,* **25,** 1842–1851, doi:10.1175/2010WAF2222406.1.

——, and H. Wang, 2009: A new approach to forecasting typhoon frequency over the western North Pacific. *Wea. Forecasting,* **24,** 974–986, doi:10.1175/2009WAF2222194.1.

——, ——, and Y.-J. Choi, 2008: A physically-based statistical forecast model for the middle-lower reaches of the Yangtze River Valley summer rainfall. *Chin. Sci. Bull.,* **53,** 602–609, doi:10.1007/s11434-008-0083-1.

——, Y. Liu, and H. P. Chen, 2012: Improving the prediction of the East Asian summer monsoon: New approaches. *Wea. Forecasting,* **27,** 1017–1030, doi:10.1175/WAF-D-11-00092.1.

Feng, J., W. Chen, C.-Y. Tam, and W. Zhou, 2011: Different impacts of El Niño and El Niño Modoki on China rainfall in the decaying phases. *Int. J. Climatol.,* **31,** 2091–2101, doi:10.1002/joc.2217.

Gao, Y., H. Wang, and S. Li, 2013: Influences of the Atlantic Ocean on the summer precipitation of the southeastern Tibetan Plateau. *J. Geophys. Res. Atmos.,* **118,** 3534–3544, doi:10.1002/jgrd.50290.

Gu, W., C. Y. Li, X. Wang, W. Zhou, and W. J. Li, 2009: Linkage between mei-yu precipitation and North Atlantic SST on the decadal timescale. *Adv. Atmos. Sci.,* **26,** 101–108, doi:10.1007/s00376-009-0101-5.

Huang, Y., H. Wang, and P. Zhao, 2013: Is the interannual variability of the summer Asian–Pacific Oscillation predictable? *J. Climate,* **26,** 3865–3876, doi:10.1175/JCLI-D-12-00450.1.

Li, X., Z. Wen, W. Zhou, and D. Wang, 2012: Atmospheric water vapor transport associated with two decadal rainfall shifts over East China. *J. Meteor. Soc. Japan,* **90,** 587–602, doi:10.2151/jmsj.2012-501.

Ma, S., X. Rodó, and F. J. Doblas-Reyes, 2012: Evaluation of the DEMETER performance for seasonal hindcasts of the Indian summer monsoon rainfall. *Int. J. Climatol.,* **32,** 1717–1729, doi:10.1002/joc.2389.

Michaelsen, J., 1987: Cross-validation in statistical climate forecast models. *J. Climate Appl. Meteor.,* **26,** 1589–1600, doi:10.1175/1520-0450(1987)026<1589:CVISCF>2.0.CO;2.

Palmer, T. N., and Coauthors, 2004: Development of a European Multimodel Ensemble System for Seasonal-to-Interannual Prediction (DEMETER). *Bull. Amer. Meteor. Soc.,* **85,** 853–872, doi:10.1175/BAMS-85-6-853.

Rong, X., R. Zhang, and T. Li, 2010: Impacts of Atlantic sea surface temperature anomalies on Indo-East Asian summer monsoon–ENSO relationship. *Chin. Sci. Bull.,* **55,** 2458–2468, doi:10.1007/s11434-010-3098-3.

Sun, B., and H. Wang, 2013: Larger variability, better predictability? *Int. J. Climatol.,* **33,** 2341–2351, doi:10.1002/joc.3582.

Sun, J., and H. Chen, 2012: A statistical downscaling scheme to improve global precipitation forecasting. *Meteor. Atmos. Phys.,* **117,** 87–102, doi:10.1007/s00703-012-0195-7.

——, H. Wang, and W. Yuan, 2009: Role of the tropical Atlantic sea surface temperature in the decadal change of the summer North Atlantic Oscillation. *J. Geophys. Res.,* **114,** D20110, doi:10.1029/2009JD012395.

Uppala, S. M., and Coauthors, 2005: The ERA-40 Re-Analysis. *Quart. J. Roy. Meteor. Soc.,* **131,** 2961–3012, doi:10.1256/qj.04.176.

Wang, H., 2001: The weakening of the Asian monsoon circulation after the end of 1970s. *Adv. Atmos. Sci.,* **18,** 376–386, doi:10.1007/BF02919316.

——, 2002: The instability of the East Asian summer monsoon–ENSO relations. *Adv. Atmos. Sci.,* **19,** 1–11, doi:10.1007/s00376-002-0029-5.

——, Y. Zhang, and X. Lang, 2010: On the predictand of short-term climate prediction (in Chinese). *Climate Environ. Res.,* **15,** 225–228.

——, K. Fan, X. Lang, J. Sun, and L. Chen, 2012: Initiating and applying the interannual increment prediction approach (in Chinese). *Advances in Climate Prediction Theory and Technique of China,* China Meteorological Press, 120–139.

Wang, X., D. Wang, W. Zhou, and C. Li, 2012: Interdecadal modulation of the influence of La Niña events on Mei-yu rainfall over the Yangtze River Valley. *Adv. Atmos. Sci.,* **29,** 157–168, doi:10.1007/s00376-011-1021-8.

Wu, J., and X. J. Gao, 2013: A gridded daily observation dataset over China region and comparison with the other datasets (in Chinese). *Chin. J. Geophys.,* **56,** 1102–1111.

Zhao, P., Y. Zhu, and R. Zhang, 2007: An Asian–Pacific teleconnection in summer tropospheric temperature and associated Asian climate variability. *Climate Dyn.,* **29,** 293–303, doi:10.1007/s00382-007-0236-y.

——, Z. Cao, and J. Chen, 2010: A summer teleconnection pattern over the extratropical Northern Hemisphere and associated mechanisms. *Climate Dyn.,* **35,** 523–534, doi:10.1007/s00382-009-0699-0.

——, B. Wang, and X. Zhou, 2012: Boreal summer continental monsoon rainfall and hydroclimate anomalies associated with the Asian–Pacific Oscillation. *Climate Dyn.,* **39,** 1197–1207, doi:10.1007/s00382-012-1348-6.

Zhao, Z., 1999: Part I: The overview (in Chinese). *Summertime Floods and Droughts in China and the Associated Circulations,* China Meteorological Press, 10–12.

Zhou, B., and P. Zhao, 2010: Influence of the Asian–Pacific oscillation on spring precipitation over central eastern China. *Adv. Atmos. Sci.,* **27,** 575–582, doi:10.1007/s00376-009-9058-7.

——, X. Cui, and P. Zhao, 2008: Relationship between the Asian–Pacific oscillation and the tropical cyclone frequency in the western North Pacific. *Sci. China,* **51D,** 380–385, doi:10.1007/s11430-008-0014-7.

——, P. Zhao, and X. Cui, 2010: Linkage between the Asian–Pacific Oscillation and the sea surface temperature in the North Pacific. *Chin. Sci. Bull.,* **55,** 1193–1198, doi:10.1007/s11434-009-0386-x.

Zhu, Y., H. Wang, W. Zhou, and J. Ma, 2011: Recent changes in the summer precipitation pattern in East China and the background circulation. *Climate Dyn.,* **36,** 1463–1473, doi:10.1007/s00382-010-0852-9.